

An Empirical Model of the Gibbs Free Energy for Solutions of NaCl and CaCl₂ of Arbitrary Concentration at Temperatures from 423.15 K to 623.15 K under Vapor Saturation Pressure¹

M. V. Ivanov^{a,*}, S. A. Bushmin^a, and Corresponding Member of the RAS L. Y. Aranovich^b

Received November 9, 2017

Abstract—An empirical model for the concentration dependence of the Gibbs free energy for solutions of chlorides of alkaline and alkaline earth metals in water is proposed. A simple analytical form of the Gibbs free energy makes it possible to obtain the equations of state for salt solutions that are equally accurate in the entire range of salt concentrations, from dilute solutions to solubility limits. The high accuracy of the thermodynamic description of solutions of high and intermediate concentration is ensured by the presence in the equation for the Gibbs free energy of two terms related to the Margules decomposition of the Gibbs free energy. Our form of the Gibbs free energy also contains a term that reproduces the thermodynamic behavior of solutions of electrolytes, which ensures high accuracy of the proposed model at low salt concentrations in the solution. Using the model, the equations of state for aqueous solutions of NaCl and CaCl₂ at water vapor pressure in the temperature ranges of 423.15 K–573.15 K and 423.15 K–623.15 K were obtained, which corresponds to the parameters of ore-bearing solutions participating in the formation of low-temperature hydrothermal ore deposits.

DOI: 10.1134/S1028334X18040141

Salts NaCl and CaCl₂ are the most common components of natural water–salt fluids. By now, for the system H₂O–NaCl, there is a significant number of sufficiently accurate and reliable thermodynamic models suitable for a wide range of geologically important temperatures and pressures. Theoretical knowledge on the system H₂O–CaCl₂ is rather poor. At the same time, CaCl₂ solubility in water at 20°C is close to the solubility of NaCl (6.7 and 6.1 mol/kg H₂O, respectively) and high concentrations of CaCl₂ are quite frequent in natural fluids [1]. It is experimentally established that carbon dioxide is less soluble in the solution H₂O–CaCl₂ in comparison with H₂O–NaCl. The above-mentioned information, together with the fact that natural fluids often contain a mixture of NaCl and CaCl₂, makes relevant the development of an adequate and mutually compatible thermodynamic description of NaCl and CaCl₂ solutions suit-

able for the whole range of possible salt concentrations. Construction of such a description is the aim of the present work.

As an initial approximation, we applied the expression for the Gibbs free energy, proposed in [2, 3], with the addition of two terms, one of which provides an adequate description of a dilute electrolyte solution, and the other of which provides the necessary accuracy of the model for concentrated solutions. This thermodynamic model is used to describe aqueous solutions of NaCl and CaCl₂ of arbitrary concentration under the vapor saturation pressure and temperature 423.15–573.15 K and 423.15–623.15 K, respectively. The chosen temperature interval corresponds, in particular, to the parameters of the hydrothermal fluids involved in the formation of epithermal, some porphyry, and most orogenic gold deposits [4]. Extension of the model to the case of higher pressures will be the subject of a future publication.

The Gibbs free energy per mole of the solution G [J/mol] looks like

$$G = G^{\text{mix}} + x_1 G_1^0 + x_2 G_2^0, \quad (1)$$

where $x_1 = x_{\text{H}_2\text{O}}$ is the mole fraction of water, x_2 is the mole fraction of salt ($x_2 = x_{\text{NaCl}}$ or $x_2 = x_{\text{CaCl}_2}$) in the solution, and G_1^0 and G_2^0 are, correspondingly, the Gibbs free energies of one mole of pure water and one

¹ The article was translated by the authors.

^a Institute of Precambrian Geology and Geochronology, Russian Academy of Sciences, St. Petersburg, 199034 Russia

^b Institute of the Geology of Ore Deposits, Petrography, Mineralogy, and Geochemistry, Russian Academy of Sciences, Moscow, 119017 Russia

*e-mail: m.v.ivanov@ipgg.ru

mole of dissolved salt at the given temperature T and pressure P . In turn, the Gibbs free energy of mixing G^{mix} consists of two parts:

$$G^{\text{mix}} = G^{\text{config}} + G^{\text{ex}}.$$

The configuration Gibbs free energy $G^{\text{config}} = G^{\text{id}} + G_{\alpha}$ is the sum of the ideal free energy of mixing of water and salt

$$G^{\text{id}} = RT(x_1 \ln x_1 + x_2 \ln x_2),$$

and a part of the free energy, dependent on degree of dissociation of the salt molecules α

$$G_{\alpha} = RT[\alpha x_2 \ln x_2 - x_1 \ln(1 + \alpha x_2) - (1 + \alpha)x_2 \ln(1 + \alpha x_2) + (1 + \alpha)x_2 \ln(1 + \alpha)], \quad (2)$$

which is analogous to that in [2, 3]. In the current work, we did not consider possible dependencies of α on the temperature, pressure, and salt concentration. We used its fixed values, corresponding to the full dissociation of the electrolyte molecules, i.e., $\alpha = 1$ for NaCl and $\alpha = 2$ for CaCl₂. The total number of ions formed due to the dissociation of one molecule of electrolyte is $\nu = \alpha + 1$.

In our thermodynamic model, the excess Gibbs free energy consists of three terms

$$G^{\text{ex}} = G_1 + G_2 + G_3. \quad (3)$$

The term of the Margules type

$$G_2 = x_1 x_2 W_2(T, P) = g_2 W_2(T, P) \quad (4)$$

was introduced in [2] as a part of a thermodynamic model of a fluid at high TP -parameters. For achieving an adequate reproduction of more detailed experimental data related to temperatures below the critical point of water, we introduced another term, which describes the thermodynamic behavior of the fluid with a high concentration of salt

$$G_3 = x_1 x_2^2 W_3(T, P) = g_3 W_3(T, P). \quad (5)$$

The contribution of the electrostatic interaction of ions, most important for dilute solutions, is described in our model by an empirical term

$$G_1 = \{x_2^{1/2} \ln(1 + x_2^{1/2}/\varepsilon_1(T, P)) - x_2 \ln(1 + 1/\varepsilon_1(T, P))\} W_1(T, P) = g_1 W_1(T, P), \quad (6)$$

which depends on two parameters ε_1 and W_1 . The first term in Eq. (6) is obtained from the requirement of precise reproduction of experimental data at low values of x_2 . The second term is necessary for satisfying the condition $G_1(x_2 = 1) = 0$. The equations for chemical potentials μ_i , activities a_i , and activity coefficients γ_i , following from our form of the Gibbs free energy (1)–(6), are given in [5].

The most convenient representation of experimental data on binary solutions at water vapor saturation

pressures is their expression through the osmotic coefficient

$$\varphi = -\frac{1000}{\nu m M_1} \ln a_1.$$

Here, M_1 is the molar mass of water, and m is the molality of the solution. The osmotic coefficient is directly associated with the difference between the pressure of the saturated vapor over the surface of pure water and the pressure over the surface of a corresponding solution at a given temperature [6]. For solutions of NaCl, smoothed dependencies $\varphi(m)$, based on data of a number of experimental studies, are obtained in [6].

For every separate value of temperature and corresponding vapor saturation pressure, our Gibbs free energy G^{mix} and, thereafter, φ are defined by four parameters W_1 , ε_1 , W_2 , and W_3 . The values of these parameters, obtained for several values of the temperature, are given in Table 1. Dependencies $\varphi(x_{\text{NaCl}})$, obtained with these parameters, reproduce precisely the data of [6] (see Fig. 1). A comparison of concentration dependencies of the osmotic coefficient, obtained in our model for G^{mix} with several widely used thermodynamic models [7, 8] is presented in Fig. 2. All the models are in good agreement with experimental data at low and intermediate concentrations of NaCl. On the other hand, at high concentrations of NaCl, our form of the Gibbs free energy is in better agreement with the experimental data and demonstrates correct asymptotic behavior φ at high values of m (or x_2). A discrepancy between theoretical and experimental values of the osmotic coefficient for high concentrations of NaCl is inherent not only in the classic thermodynamic models by Pitzer and Archer [7, 8], but also in the most modern models, such as [9, 10], which are also less precise compared to our model. The high precision of the approximation of the experimental data in our model is provided by the presence in Eq. (3) of the terms G_2 and G_3 , analogous to the first terms of the Margules decomposition of the Gibbs free energy.

The data of Table 1 facilitate finding empirical temperature dependencies for the parameters W_1 , ε_1 , W_2 , and W_3 . The adequacy of such dependencies should be checked by means of fitting the total set of experimental data on $\varphi(x_{\text{NaCl}}, T)$ over the whole range of temperatures 423.15–573.15 K. The following form of these dependencies was found to be satisfactory for this fit:

$$W_1(T) = W_{1T} = (T/u_{10})^{7/2}, \quad (7)$$

$$\varepsilon_1(T) = u_{\varepsilon 0} + u_{\varepsilon 2}(T - u_{\varepsilon 1})^2 T, \quad (8)$$

$$W_2(T) = W_{2T} = u_{20} + u_{22}(T - u_{21})^2 T^{3/2}, \quad (9)$$

$$W_3(T) = W_{3T} = u_{30} + u_{32}(T - u_{31})^2 T^{3/2}. \quad (10)$$

The values of the parameters of these equations for NaCl solutions at temperatures of 423.15–573.15 K are given in Table 2. These values are obtained by fitting a number of φ values for various temperatures and mole fractions of NaCl from [6]. In the limits of precision of the graphical representation of data, the dependencies $\varphi(T)$, obtained with these parameters, are not distinguishable from the dependencies shown in Fig. 1.

The second system we discuss is a much less theoretically studied system, H₂O–CaCl₂. Since the solubility of CaCl₂ in water is slightly higher than the solubility of NaCl, the limitations inherent in the existing thermodynamic models are even more pronounced for the H₂O–CaCl₂ system (e.g., the model of [11]) compared to H₂O–NaCl. To construct the thermodynamic model of the H₂O–CaCl₂ system in the temperature range 423.15–623.15 K at the saturated vapor pressure, we used the same form for the Gibbs free energy as for H₂O–NaCl with temperature-dependent parameters in the form of (7)–(10). The experimental data were taken from [12–14]. The values of the osmotic coefficient obtained from these data were used for the numerical fit of the parameters of Eqs. (7)–(10). The adjusted values of the parameters are given in Table 2. Our theoretical curves $\varphi(x_{\text{CaCl}_2})$ for several temperatures together with the corresponding experimental points are shown in Fig. 3.

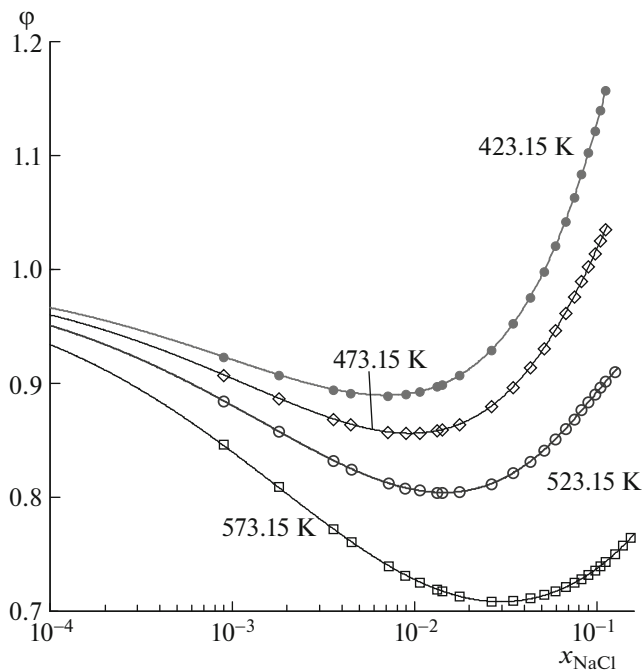


Fig. 1. Osmotic coefficient φ dependent on the mole fraction of NaCl in a water solution under saturated vapor pressure. Experimental points [6] and our theoretical curves with the parameters of Table 1.

Table 1. Parameters of the thermodynamic model (1)–(6) for H₂O–NaCl under vapor saturation pressure at several values of the temperature

T, K	$W_1 \times 10^{-3}$	$\varepsilon_1 \times 10^2$	$W_2 \times 10^{-3}$	$W_3 \times 10^{-3}$
423.15	0.8347143	8.6195923	-29.197709	-2.1073137
448.15	1.0225891	8.9419517	-20.865319	6.4245873
473.15	1.2327865	9.1740687	-14.189644	12.244419
498.15	1.4836048	9.3799913	-8.8302268	15.809539
523.15	1.7448823	9.4042367	-7.1058428	14.003259
548.15	2.0564525	9.3578519	-8.4561929	7.5919937
573.15	2.4123808	9.1395501	-15.137043	-6.5520859

The experimental results [12, 13] relate to the concentrations of the CaCl₂ solution below the solubility limit at $T = 373.15 \text{ K}$. On the other hand, most data [14] refer to more concentrated solutions, the preparation of which is possible only at pressures above atmospheric pressure. In Fig. 3, we see very good agreement between all three groups of experiments among themselves and the results of our thermodynamic model with experimental data. The mutual agreement of the experimental data relating to different concentration ranges and different requirements for the experiment was the basis for our choice in favor of the experimental data of [12–14]. On the other hand, the experimental data of [15] are significantly different from the results of other studies in the field of moderate concentrations of CaCl₂ and significantly change their behavior when passing through the solubility limit at

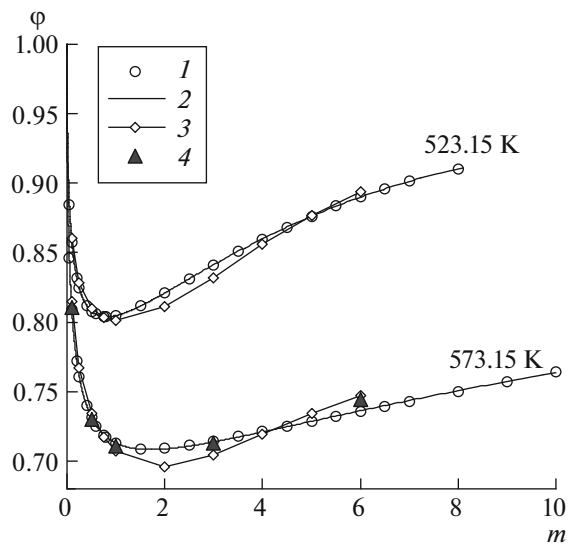


Fig. 2. Osmotic coefficient at the saturated vapor pressure dependent on molality m of the solution H₂O–NaCl. Our results (2) compared with experimental data [6] (1) and models by Pitzer [7] (3) and Archer [8] (4).

Table 2. Numerical parameters defining the temperature dependence of the Gibbs free energy for the pressure of the saturated vapor

u	$\text{H}_2\text{O}-\text{NaCl}$	$\text{H}_2\text{O}-\text{CaCl}_2$
u_{10}	6.19119130×10^1	4.20228033×10^1
u_{e0}	$9.44196901 \times 10^{-2}$	$1.00583446 \times 10^{-1}$
u_{e1}	5.22720408×10^2	5.76519936×10^2
u_{e2}	$-2.05279225 \times 10^{-9}$	$-7.17994571 \times 10^{-10}$
u_{20}	-7.40465984×10^3	-2.77768788×10^4
u_{21}	5.26013556×10^2	5.44377081×10^2
u_{22}	$-2.32223423 \times 10^{-4}$	$-5.81597173 \times 10^{-5}$
u_{30}	1.51261293×10^4	1.08900613×10^4
u_{31}	5.02648252×10^2	6.98424638×10^2
u_{32}	$-3.04159146 \times 10^{-4}$	$1.95356143 \times 10^{-4}$

$T = 373.15$ K. Therefore, they were not included in the calculation of the parameters in Table 2.

The thermodynamic model of the Gibbs free energy, presented above, allowed us to describe with a high precision the behavior of two geologically significant fluid systems $\text{H}_2\text{O}-\text{NaCl}$ and $\text{H}_2\text{O}-\text{CaCl}_2$ at a saturated vapor pressure in the temperature range from 423.15 K to temperatures approaching the critical point of water and in a wide range of concentrations up

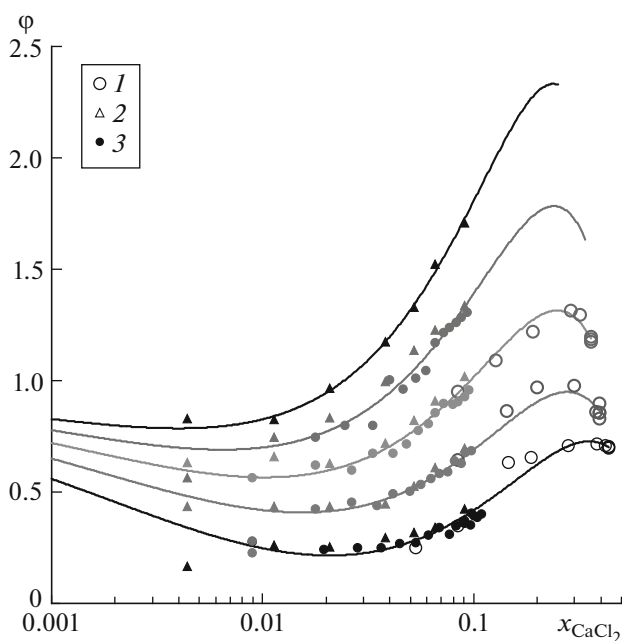


Fig. 3. Osmotic coefficient ϕ dependent on the mole fraction of CaCl_2 in water solutions under saturated vapor pressure. Experimental points and our theoretical curves at $T = 423.15, 473.15, 523.15, 573.15,$ and 623.15 K (top downwards). 1—[14], 2—[12], 3—[13].

to saturation. In the future, the model will be extended to pressures up to several kilobars while obtaining the $PVTx$ characteristics of the systems. The extended model will be used as an integral part in modeling more complex fluids containing nonpolar gases.

Upon request, the authors can provide a computer program that implements calculations according to the thermodynamic model presented above.

ACKNOWLEDGMENTS

This research was carried out within the framework of the research program at the Institute of Precambrian Geology and Geochronology, Russian Academy of Sciences, project no. 0153-2018-0004, and was supported by the Russian Foundation for Basic Research, project no. 18-05-00058.

REFERENCES

1. J. L. Bischoff, R. J. Rosenbauer, and R. O. Fournier, *Geochim. Cosmochim. Acta* **60**, 7–16 (1996).
2. L. Ya. Aranovich, I. V. Zakirov, N. G. Sretenskaya, et al., *Geochem. Int.* **48** (5), 446–455 (2010).
3. L. Y. Aranovich and R. C. Newton, *Contrib. Mineral. Petrol.* **125**, 200–212 (1996).
4. N. S. Bortnikov, *Geol. Ore Deposits* **48**, 1–22 (2006).
5. M. V. Ivanov and S. A. Bushmin, *Cornell Univ. Library*, 2017. arXiv:1705.02901v2 [physics.chem-ph], pp. 1–26.
6. C. Liu and W. T. Lindsay, Jr., *J. Solution Chem.* **1**, 45–69 (1972).
7. K. S. Pitzer, J. C. Peiper, and R. H. Busey, *J. Phys. Chem. Ref. Data* **13**, 1–102 (1984).
8. D. G. Archer, *J. Phys. Chem. Ref. Data* **21**, 793–829 (1992).
9. R. Sun and J. Dubessy, *Geochim. Cosmochim. Acta* **88**, 130–145 (2012).
10. F. F. Hingerl, T. Wagner, D. A. Kulik, et al., *Chem. Geol.* **381**, 78–93 (2014).
11. K. S. Pitzer and C. S. Oakes, *J. Chem. Eng. Data* **39**, 553–559 (1994).
12. V. I. Zarembo, S. N. L'vov, and M. Yu. Matuzenko, *Geokhimiya*, No. 4, 610–614 (1980).
13. S. A. Wood, D. A. Crerar, S. L. Brantley, et al., *Am. J. Sci.* **284**, 668–705 (1984).
14. V. A. Ketsko, M. A. Urusova, and V. M. Valyashko, *Zh. Neorg. Khim.* **29**, 2443–2445 (1984).
15. M. S. Gruskiewicz and J. M. Simonson, *J. Chem. Thermodyn.* **37**, 906–930 (2005).